

CO5-1 Determination of Particulate, Inorganic and Organic Gaseous Halogens in the Atmosphere

H. Tsukada, A. Takeda, H. Kakiuchi and N. Akata

Department of Radioecology,
Institute for Environmental Sciences

INTRODUCTION: Chemical species of atmospheric halogens are classified into particulate, inorganic and organic forms. We applied a simple method for determination of particulate, inorganic and organic gaseous halogens in the atmosphere by means of simultaneously sampling at three types of filters. In this study, we reported simple method for sampling and analysis of particulate, inorganic gaseous and organic gaseous halogens, Cl, Br and I, in the atmosphere.

EXPERIMENTS: The sampling system consisted of nine filters of 47 mm ϕ , which were supported in NILU filter holders (NL-0-009) connected in a series (Figure 1). Fine and coarse particulate halogens were separately collected with fluoropore filters (AF07P, Sumitomo Electric; DOP: 0.3 μm , collection efficiency: 99.99%) by cascade impactor and backup stage. Inorganic gaseous halogens were sampled with three cellulose filters (Whatman 41) impregnated with 1 M LiOH in a 10% glycerol water mixture[1]. Organic gaseous halogens were absorbed in three activated carbon paper filters (STV-505, Kynol). Outdoor sample air was passed at the flow rate of 10 L min^{-1} during approximately two weeks. After sample collection, each filter sample was separately sealed in a polyethylene bag, and analyzed for Cl, Br and I by neutron

activation analysis using the KUR reactor (Pn-3) at a thermal neutron flux rate of $4.9 \times 10^{16} \text{ n m}^{-2} \text{ s}^{-1}$ for 150 s.

RESULTS: Table 1 shows the collection efficiencies of inorganic and organic gaseous halogens calculated with three stages. The collection efficiencies of inorganic and organic I ranged from 82.1 to 93.4% with a mean of $87.5 \pm 4.9\%$ and from 91.3 to 100.0% with mean of $96.6 \pm 3.6\%$, respectively. And collection efficiencies of inorganic and organic Br ranged from 100.0 to 101.7% with mean of $100.3 \pm 0.3\%$ and from 80.2 to 93.4% with mean of $88.5 \pm 5.4\%$, respectively. Inorganic and organic Cl were collected 100% by this system, because Cl of each third stage filters weren't detected. Although the collection efficiency of I is the lowest among halogens, recoveries of inorganic and organic gaseous I in this system were more than 80%. And, atmospheric concentrations of course ($> 2.0 \mu\text{m}$) and fine ($< 2.0 \mu\text{m}$) particulate I, inorganic and organic gaseous I from September to December 2006 ranged 0.17 to 0.52, 0.46 to 1.38, 1.50 to 3.44 and 1.66 to 5.94 ng m^{-3} , respectively. We clarify the seasonal variation of each chemical form of halogens in the atmosphere and inorganic gas-fine particle conversion in future studies.

REFERENCES:

- [1] K.A. Rahn, R.D. Borys, R.A. Duce, Science, 192 (1976) 549

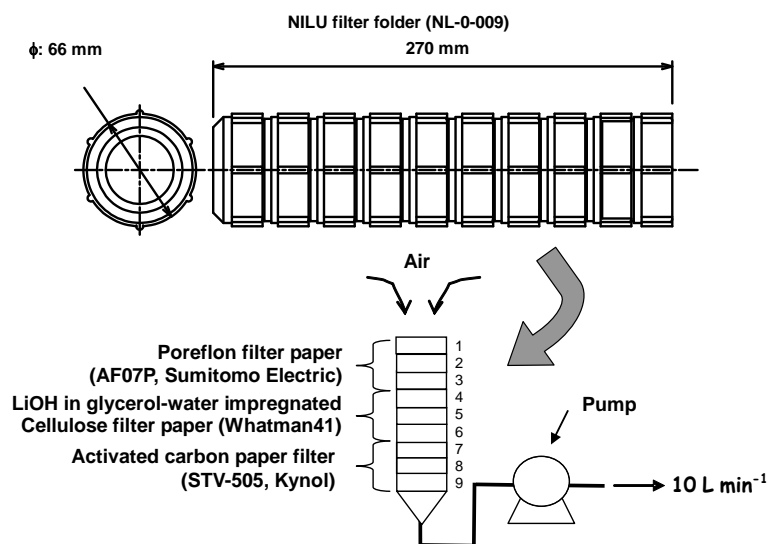


Fig.1 Configuration figure of routine air sampling system by NILU filter folder with cascade impactor

Table 1 Collection efficiencies (%) of inorganic and organic gaseous halogens (n=5)

	Inorganic			Organic		
	Range	Mean \pm S.D.		Range	Mean \pm S.D.	
I	82.1 - 93.4	87.5 ± 4.9		91.3 - 100.0	96.6 ± 3.6	
Br	100.0 - 101.7	100.3 ± 0.8		80.2 - 93.4	88.5 ± 5.4	
Cl	100.0	100.0		100.0	100.0	

N. Hasebe, K. Ito, S. Ohishi¹ Y. Nakano¹ and M. Ogata²

Institute of Nature and Environmental Technology, Kanazawa University

¹*Graduate School of Natural Science and Technology, Kanazawa University*

²*College of Science and Engineering, Kanazawa University*

INTRODUCTION: Luminescence dating observes the natural accumulated radiation damage caused by radioisotopes such as U and Th as the form of glow after stimulation by heating or lightening. The luminescence is observed at various wavelengths and emission color of luminescence can be recorded easily by using thermoluminescence color image (TLCI) analysis for samples artificially irradiated with gamma-rays [1]. TLCI information is then used to set luminescence dating protocol. To date calcite veins within bentonite deposit distributed in Luzon, Philippines, where geological processes expected in a deep geological repository of radioactive wastes from nuclear reactors are observed in natural condition, TLCI was obtained and luminescence dating was performed.

SAMPLES: A deep geological repository of radioactive wastes from nuclear reactors is composed of several barriers including cement and bentonite. High alkaline groundwater might be produced through the alternation of the cement, thus the stability of bentonite during the interaction with high alkaline groundwater is one of the important issues to be studied as bentonite plays an important role to prevent an outflow of the contaminated groundwater to the environment owing to its cation exchange and swelling properties.

To understand bentonite-alkaline groundwater reaction with the geological timescale, it is useful to investigate a similar phenomenon occurred in nature. There is an ophiolite suites covered with bentonite layer in Luzon, Philippines. High alkaline groundwater originated probably from the serpentinization of mafic rocks has been circulating along cracks in a rock and bentonite layers [2]. To determine the timescale of fluid-bentonite interaction, calcite precipitated from high alkaline groundwater was dated using the thermoluminescence dating method.

EXPERIMENTS: First, thermoluminescence color of calcite samples was investigated. Samples were irradiated by gamma-ray from Co-60 with dose rate of about 1.467kGy/h at Kyoto University Research Reactor Institute. The total gamma dose were 36 kGy given for 24.5 hours on the irradiation stage, which stand off 20cm from the radiation source. They emit red luminescence. Paleodose was measured using this red thermoluminescence

and SARA (single-aliquot regeneration and added dose [3]) method was applied to evaluate sensitivity change of calcite occurred through repeated heating of samples. In annual dose measurement, we measured radioactive element concentrations of calcite and a surrounding mafic sample using XRF, EPMA, LA-ICP-MS analyses. A cosmic ray contribution to annual dose was calculated by an equation of [4].

To know the annual dose of a heterogeneous sample, detailed three-dimensional rock distributions around the sample is necessary. Unfortunately, the analyzed sample was very small in size, therefore we do not know accurate distribution of surrounding rock facies. By assuming the ratio of calcite and the surrounding mafic rock, the age of calcite was calculated (Fig.1).

RESULTS: The order of calcite age is ~10ka (younger than 100ka and older than 20ka). For accurate dating, it is necessary to consider errors in added dose, exact distribution of rock which contributes the annual dose, and development of a method to estimate an annual dose for a heterogeneous sample.

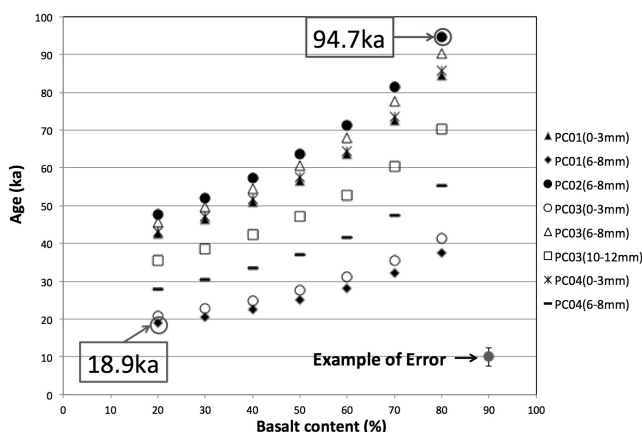


Fig. 1. Age estimates under the assumption of basalt content.

REFERENCES:

- [1] T. Hashimoto et al., Nucl. Tracks, **16** (1989) 3-10.
- [2] E.E. Geary, R.W. Kay, J.C. Reynolds and S.M. Kay, Tectonophysics, **168** (1989) 43-63.
- [3] V. Mejdahl and L. Bøtter-Jensen, Quat. Sci. Rev., **13** (1994) 551-554.
- [4] J.R. Prescott and J.T. Hutton., Rad. Meas., **23** (1994) 497-500.

CO5-3 Determination of Trace Amount of Cl, Br and I in Sedimentary Rock Samples

M. Ebihara and S. Sekimoto¹

Graduate School of Science, Tokyo Metropolitan University

¹Research Reactor Institute, Kyoto University

INTRODUCTION: It is important to know the elemental composition in meteorite samples for discussing the classification, formation mechanism and metamorphism of those samples in terms of cosmochemistry. However, the behavior of Cl, Br and I, that is, the halogen elements in the formation and metamorphism of meteorites have rarely been studied in detail because accurate and reliable data about the abundances of the halogens, which mean Cl, Br and I hereafter, in meteorites have scarcely been obtained.

The shortage of accurate and reliable data about the abundances of halogens in cosmochemical and also geological samples is due to difficulty in determination of trace amount of halogen elements by using convenient and/or conventional analytical method. In igneous rocks and sedimentary rocks, which are commercially available in National Institute of Advanced Industrial Science and Technology, generally their Cl, Br and I contents were reported as only preferable values or have never been reported.

In this work, trace amount of Cl, Br and I were determined by radiochemical neutron activation analysis (RNAA) using Kyoto University Reactor (KUR) in geochemical reference samples, "Sedimentary rock series" where recommended values are not given, but preferable values are only given. Since, in sedimentary rock series, only preferable values have been reported by Imai et al. [1] for Cl, and only those preferable values [1] and experimental values using ICP-MS by Chai and Muramatsu [2] for Br and I, it is very meaningful to present reliable value of Cl, Br and I using RNAA, which has never been used for analysis of sedimentary rocks.

EXPERIMENTS: Trace amount of Cl, Br and I in sedimentary rocks and rhyolite samples were determined by (RNAA). The preparation of reference chemical standards, the neutron irradiation, the radiochemical separation scheme, the chemical yield determination and the data reduction for RNAA used in this work were essentially the same as that described in Ebihara and Sekimoto [3].

RESULTS: In the nine sedimentary rocks and the three rhyolite samples, Cl, Br and I contents were determined three to five times independently within the uncertainties of 2-13% for Cl, 3-13% for Br and 2-22% for I, respectively. The uncertainties quoted in the above Cl, Br and I contents mainly depend on counting statistics in the γ -ray measurements. The original data obtained by three to five times RNAA in each sample are transformed, by

variance analysis, into a new set of values with uncertainties of one standard deviation, which are shown in Table 1. The halogen contents of the three rhyolites (JR-1, JR-2 and JR-3) obtained in this work are approximately consistent with the previous values by RNAA using the JRR-4 reactor of the Japan Atomic Energy Agency, whose thermal neutron flux is $3.2 \times 10^{13} \text{ n cm}^{-2} \text{ s}^{-1}$ under 3.5MW operation [4]. In spite of the reactor characteristics and the irradiation conditions; thermal neutron flux, irradiation time and so on, it is confirmed that the results of RNAA for the halogens is reproducible. We expect that the halogen contents in the nine sedimentary rocks are successfully obtained by RNAA in this work.

Comparing the halogen contents of the nine sedimentary rocks obtained in this work to the preferable values reported by Imai et al. [Z], our analytical values tend to be lower than the preferable values except for Br contents in JSd-1 and JSd-3. Since those preferable values are the compiled data provided by only two or three independent determination, the confidence level of those data is low. Our analytical values with the uncertainties of 2-22% are much more reliable than those preferable values.

Table 1. Measured contents of Cl, Br and I in the nine sedimentary rocks and three rhyolites

Sample	Cl (ppm)	Br (ppm)	I (ppb)
JLk-1	59±2	7.83±0.53	9090±640
JLs-1	17±2	105±12 ppb	319±29
JDo-1	36±6	623±50 ppb	789±39
JSL-1	14±2	123±15 ppb	108±8
JSL-2	7.58±0.74	60±6 ppb	97±9
JSd-1	64±7	1.85±0.1	1090±90
JSd-2	23±2	1.13±0.04	674±63
JSd-3	26±1	3.92±0.08	4220±330
JCh-1	4.75±0.25	27±5 ppb	115±13
JR-1	982±71	2.07±0.06	84±3
JR-2	789±39	1.64±0.12	86±15
JR-3	134±12	0.577±0.045	482±37

REFERENCES:

- [1] N. Imai et al., Geostandards Newsletter, 20, 165-216 (1996).
- [2] J.Y. Chai and Y. Muramatsu, Geostandards and Geoanalytical Research, 31, 143-150 (2007).
- [3] M. Ebihara and S. Sekimoto, KURRI PROGRESS REPORT (2010) CO5-9
- [4] H. Ozaki and M. Ebihara., Anal. Chim. Acta 583, 384-391 (2007).

K. Ninagawa

Department of Applied Physics, Okayama University of Science

TL OF ORDINARY CHONDRITES: Induced TL (thermoluminescence), the response of a luminescent phosphor to a laboratory dose of radiation, reflects the mineralogy and structure of the phosphor, and provides valuable information on the metamorphic and thermal history of meteorites. Especially the sensitivity of the induced TL is used to determine petrologic subtype of unequilibrated ordinary chondrites [1]. Natural TL, the luminescence of a sample that has received no irradiation in the laboratory, reflects the thermal history of the meteorite in space and on Earth. Natural TL data thus provide insights into such topics as the orbits of meteoroids, the effects of shock heating, and the terrestrial history of meteorites [2]. Natural TL properties are usually applied to find paired fragments [3-5]. This time we measured induced and natural TL properties of twenty-eight Yamato unequilibrated ordinary chondrites (LL3: 2, L3: 12, H3: 14) from Japanese Antarctic meteorite collection. Sampling positions of these chondrites were measured by GPS.

PRIMITIVE ORDINARY CHONDRITES: Most of the chondrites had TL sensitivities over 0.1 (Dhajala=1), corresponding to petrologic subtype 3.5-3.9. Four chondrites, Y982042 (L3), Y982240 (L3), Y981664 (H3) and Y981744 (H3) were revealed to be primitive ordinary chondrites as shown in Fig.1, petrologic subtype 3.2, 3.3, 3.2-3.3 and 3.4, respectively. It is particularly significant in understanding the nature of primitive material in the solar system.

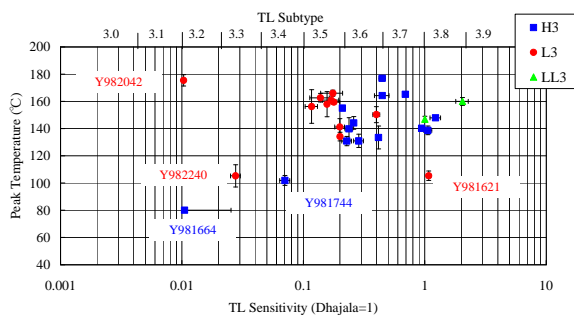


Fig.1. Induced Peak Temperature vs. TL Sensitivity to search primitive ordinary chondrites

ENSTATITE CHONDRITE: Fe-poor forsterite, Fe-poor enstatite and feldspar in meteorites have a phosphorous characteristics to exhibit the cathodoluminescence (CL) [6]. Y-86004 (EH melt rock) was reported that it had CL zoning [7]. Fig.2 shows it's color CL image.

Purple, blue, and red CL were recognized from inner side to outside with concentric structure. Moreover, there is a black layer of fusion crust at outermost region. It is suggested that this structure was made by heating during atmospheric passage from occurrence of the fusion crust. This time we measured raman spectra of the Y-86004. The results were shown in Fig 3. The minerals, which showed these Purple, blue, and red CL, were all enstatite.

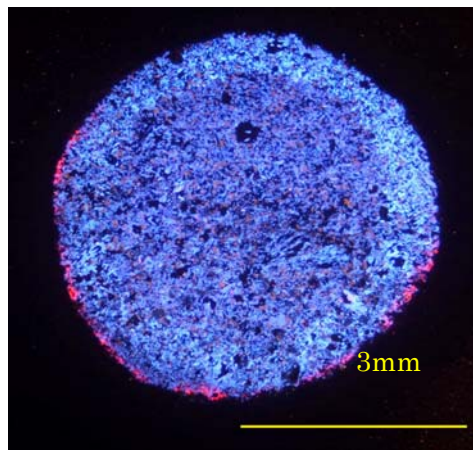


Fig.2. CL color image of Y-86004.

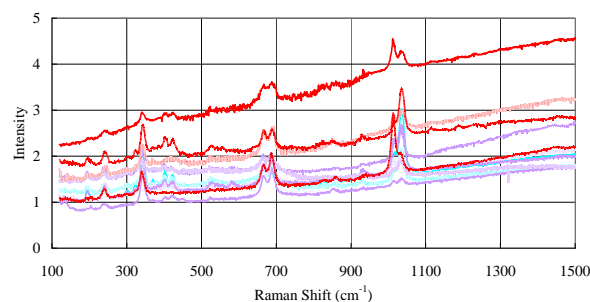


Fig.3. Raman spectra of the Y-86004.

REFERENCES:

- [1] D. W. G. Sears et al. 1991. Proceedings of Lunar and Planetary Science 21:493-512.
- [2] P. H. Benoit et al. 1991. Icarus 94: 311-325.
- [3] K. Ninagawa et al. 1998. Antarctic Meteorite Research 11:1-17.
- [4] K. Ninagawa et al. 2002. Ant-arctic Meteorite Research 15:114-121.
- [5] K. Ninagawa et al. 2005. Antarctic Meteorite Research 18:1-16.
- [6] Steele (1990): In Spectroscopic characterization of minerals and their surfaces. (ed. Coyne et al.), pp. 150-164. American Chemical Society.
- [7] K. Ninagawa et al., 2000. 25th Symposium on Antarctic Meteorites (NIPR, Tokyo), 114-116.

CO5-5 Size Distribution of Metal Elements in the Atmospheric Aerosols at Sakai, Osaka

N.Ito, A.Mizohata and Y. Nakano¹

Radiation Research Center, Osaka Prefecture University,
¹Research Reactor Institute, Kyoto University

The fine particle in the atmosphere in which some elements are toxic and can enter the human lung causes the healthy effects. So we observed the element in the fine particles at Sakai, Osaka. This report shows the size distribution of V, Ni, Zn, the concentration ration of fine and coarse particles and the difference of concentration between the soil and particles.

Table 1. Analysis factors in neutron activation analysis using KUR

Elements	Irradiation System	Irradiation time sec
V, Al, Ca, Cl, Mn	PN1	120
Na, K, Cr, Fe, Ni, Zn	PN2	7200

The particles in the atmosphere were collected by the low pressure Andersen sampler with which the particles were separated on 13 stage by the particle size. The sampler

have collected the samples in 2 weeks at Osaka Prefecture University, Sakai, Osaka. 4 samples which were collected in 2011 were analyzed for the element concentrations by the neutron activation analysis using Kyoto University Nuclear Reactor (Table 1). The gamma-rays emitted from irradiated samples were measured by Ge solid state detector and 4096 channel pulse height analyzer system.

In this report we show the results of the size distribution on V, Cr and Zn in the aerosols that were collected in May 2011 at Sakai, Osaka (Fig.1). The median of these is located at the fine particle range (<2.1 μ m) and these medians differ in the position, 0.21~0.51 μ m (V), 0.13~0.21 μ m (Ni) and 0.51~0.22 μ m (Zn).

We compare the ratios of these elements between the average in soil and the ratios in the coarse (>2.1 μ m) and fine particles (<2.1 μ m) (Fig.2). The ration of V, Cr, Ni and Zn to Fe in the soil are less than 1/500. By the contrast in the aerosols, the ration raise more than 2 times, especially Zn raises more than 10 times. This raise could be caused by the metallic fine particles from the metal product industry, the incinerator or oil burning.

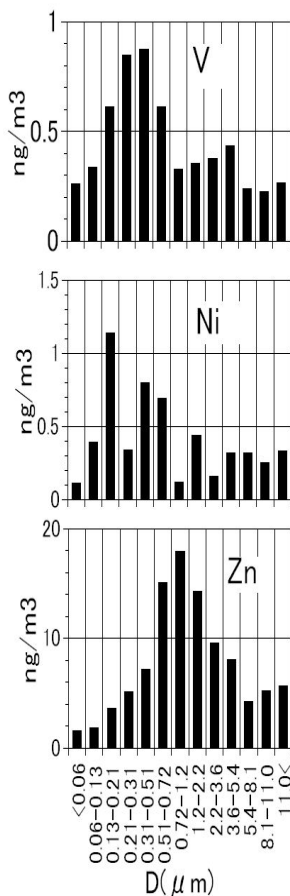


Fig.1 Size distribution of V, Ni, Zn observed at Sakai, May 2011.

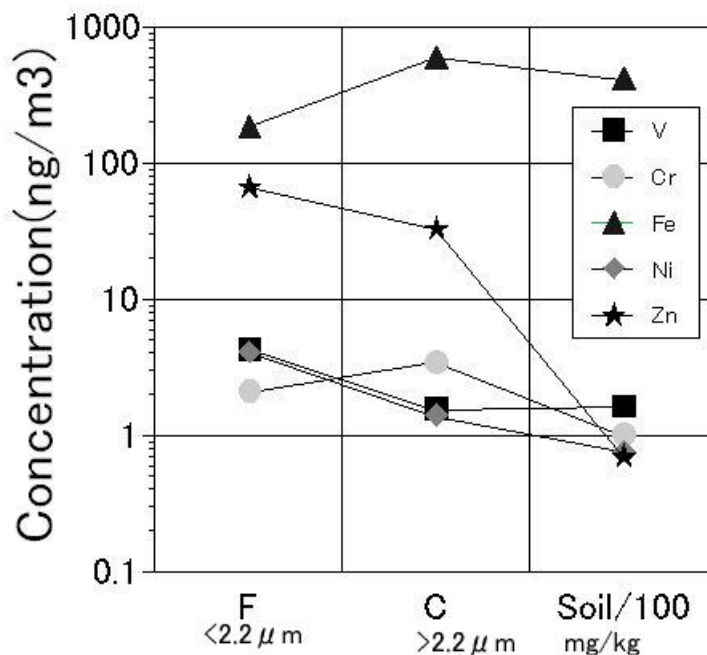


Fig.2 Concentration changes of element for the fine (F), coarse (C) and soil.

CO5-6 Estimation of Fe Vacancies of Natural Magnetite in San'in Coast Region by Mössbauer Spectra

H. Matsuyama, K. Shinoda and Y. Kobayashi¹

Department of Geosciences,
Graduate School of Science, Osaka City University
¹Research Reactor Institute, Kyoto University

INTRODUCTION: Magnetite is a typical magnetic mineral which is widely included in natural rocks and sands. The crystal structure of magnetite is inverse spinel type. Chemical compositions of magnetite vary from $[\text{Fe}^{3+}]^A[\text{Fe}^{3+}, \text{Fe}^{2+}]^B\text{O}_4$ to $[\text{Fe}^{3+}]^A[\text{Fe}^{3+}_{5/3}, \square_{1/3}]^B\text{O}_4$, where \square indicates vacancy in B site. Since the vacancy is controlled by oxygen fugacity, quantitative analyses of vacancy of natural magnetite are of interest to estimate rock's environments. Experimental methods to measure vacancies of magnetite are X-ray diffraction analyses and Mössbauer spectra measurements. In this study, vacancies of natural magnetites included in granites and sands distributed in San'in coast region of South-West Japan are estimated from X-ray and Mössbauer analyses.

EXPERIMENTS: Natural magnetites in San'in region of 18 different localities were separated. The occurrences of natural magnetite are fresh granite, weathered granite, river sand and sea sand. Chemical compositions of 18 natural magnetites were measured using SEM-EDS.

TiO_2 and Al_2O_3 were detected as solid solution components. Mössbauer spectra of natural magnetite were measured at Seto Lab. Powdered magnetite of 10mg were mixed well with powdered agarose of 100mg and pressed into a pellet. The pellet was exposed to γ -ray generated from ^{57}Co for 24 hours. By fitting the measured spectra by Lorentz function, peak area due to Fe in A and B sites are calculated. Vacancy ratio was estimated from the ratio of peak area of A and B sites. In the estimation of vacancies of natural magnetite, which often contain TiO_2 , it was assumed that the ulvöspinel component do not contribute to the magnetic splitting.

RESULTS:

Fig.1 indicates vacancies in mol% of 18 magnetites. Numbered samples are from granite. Last 3 samples are from river sand and 2 sea sands, respectively. Circled plots are from weathered occurrences judged by their appearances. All 18 samples showed vacancies below 10%. Among 18 samples, magnetites in weathered occurrence tend to show slightly high vacancy as much as 5%. In contrast, magnetites in fresh granite tend to show very low vacancy. This results imply that vacancy in magnetite is a possible indicator of weathering of rocks.

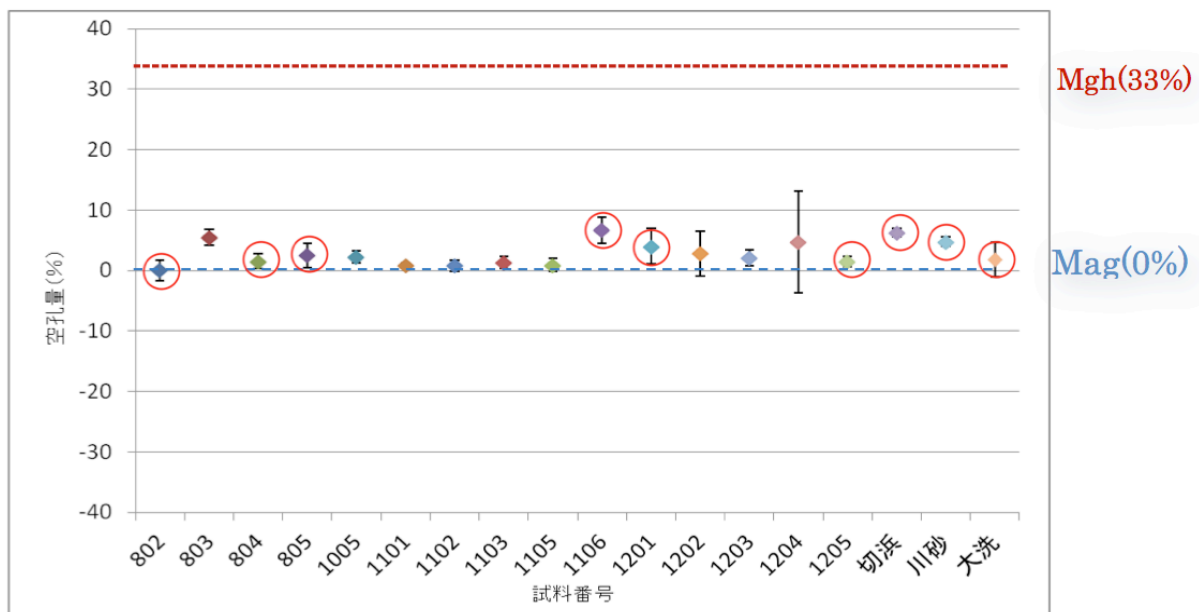


Fig.1

Fig.1 vacancies of natural magnetites in San'in coast region.

Determination of Abundance of Rare Metal Elements in Seafloor Hydrothermal Ore Deposits by INAA Techniques

J. Ishibashi, M. Ooki, T. Yamanaka¹, Y. Furuzawa¹,
T. Noguchi², R. Okumura³ and K. Takamiya³

Faculty of Science, Kyushu University

¹Faculty of Science, Okayama University

²Center for Advanced Marine Core Research,

Kochi University

³Research Reactor Institute, Kyoto University

INTRODUCTION: To meet recent increased demand for rare metal elements as mineral resources, high sensitive multi-element analysis becomes more important as geochemical tools for mineral exploration. Instrumental neutron activation analysis (INAA) has the advantage of non-destructive analysis and is free from problems that concentrate of a specific element is often included in residue during acid dissolution. Previous studies have demonstrated that INAA enables rapid abundance determination for multi elements in ore samples collected from active seafloor hydrothermal fields that consist of variety of sulfide/sulfate/silicate minerals [1,2]. In order to extend the range of application of this technique, we started preliminary studies using samples of hydrothermal sulfides and hydrothermal sediment.

EXPERIMENTS: Two groups of natural samples were provided for this study. One was hydrothermal sulfide/sulfate ores collected from active hydrothermal fields in the Okinawa Trough, and the other was hydrothermal sediments collected from Wakamiko submarine crater in the Kagoshima Bay.

For analysis of long-lived nuclides (^{110m}Ag, ⁵⁹Fe, ²⁰³Hg, ¹²⁴Sb, ⁶⁵Zn) and mid-lived nuclides (⁷⁶As, ¹⁹⁸Au, ¹³¹Ba), samples were irradiated at Pn-1 (thermal neutron flux = 3.86×10^{12} n/cm²/sec at 1 MW) for 4 hours, and the gamma ray activity was measured for 3 hours after around 30 days cooling and for 50 minutes after 3-10 days cooling, respectively. For analysis of short-lived nuclides (⁶⁶Cu, ⁵⁶Mn), samples were irradiated at Pn-3 (thermal neutron flux = 4.86×10^{12} n/cm²/sec at 1 MW) for 1-3 minutes, and the gamma ray activity was measured for 5 minutes after 10-30 minutes cooling. Concentration of each element was calculated by comparison of gamma ray intensities between the sample and standard materials; Na for short-lived nuclides measurement and Co for mid- and long-lived nuclides measurement.

RESULTS: Fig. 1 shows compilation of abundance of gold (Au) and silver (Ag) in ore samples collected from seafloor hydrothermal fields. Results obtained by this study well agree with previous studies [1,2]. Not a few ores from the Okinawa Trough showed notable enrichment in silver (Ag).

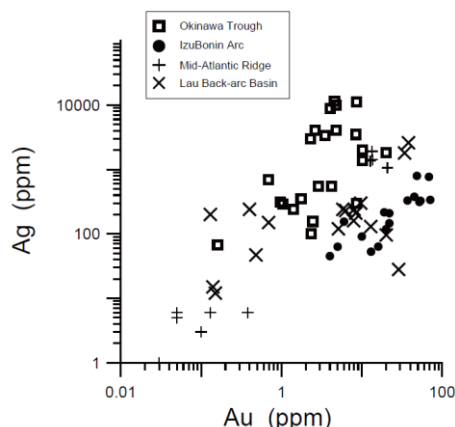


Fig. 1 Abundance of Au and Ag in ore samples collected from active hydrothermal fields in the Okinawa Trough, with data compilation from other active hydrothermal fields.

Fig. 2 shows an example of vertical profiles of elemental abundance in hydrothermal sediment collected from Wakamiko crater. The profile of gold (Au) content showed good correlation with those of arsenic (As) and antimony (Sb).

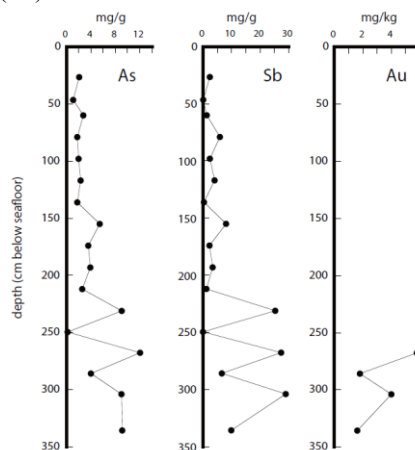


Fig. 2 Vertical profiles of As, Sb and Au concentrations in sediment samples collected from Wakamiko submarine crater.

As demonstrated above, INAA provided useful information for discussion on potential of mineral resources in a seafloor hydrothermal field.

REFERENCES:

- [1] T. Noguchi *et al.*, *Geochem. J.* 41, 141-148 (2007)
- [2] T. Noguchi *et al.*, *J. Mineral. Petrol. Sci.*, 106, 26-35 (2011)

CO5-8 ESR Study on γ -Irradiated Agricultural Wastes for Arsenic Absorber

M. Minagawa, M. Shimizu, and N. Sato¹

Graduate School of Science and Engineering, Yamagata University

¹Research Reactor Institute, Kyoto University

INTRODUCTION: We have conducted the following two different experiments emerging from previous cooperative venture in this period: (1) solid state polymerization of acrylonitrile (AN) by electron bombardment (EB) and (2) γ -irradiation on wasted agricultural products. In this report, we describe the latter topic selectively. Since some agricultural wastes are known to absorb hazardous molecules such as Arsenic (As), this topic has serious meaning from a point of view of environmental science in the 21st century. Our previous studies revealed that γ -irradiation enhances such capability. Here we report ESR results of γ -irradiated agricultural wastes to investigate the effect of radical concentration.

EXPERIMENTS: Three kinds of agricultural products were used (rice chaff, its heat-treated one, and green tea). These were packed in glass bottle and γ -irradiated at room temperature in Koga Isotope Co. Ltd. (Shiga Prefecture). The total irradiation dose rate was 100 and 200 kGy. ESR measurements were carried out by ESR spectrometer installed at KURRI to estimate the radical concentration in the bulk sample, the extent of which is directly proportional to the adsorption capacity of poisonous As contained in contaminated drinking water from the earth (underground) [1]. As adsorption property was evaluated by using color identification test established by Merck Co. Ltd.

RESULTS AND DISCUSSION: When the agricultural products were heated up to a high temperature (>400 °C) under imperfect oxidative conditions by using an electric furnace, they turned from yellow to black in its color with the increase of temperature. The radical concentration was evaluated in terms of a calibration curve of ESR (DPPH/KBr, internal standard). That is, the radical concentration was dependent strongly on the heating rate employed. In general, the slower the heating rate, the higher the radical concentration, up to the heating upper-limit 400 °C. Other independent experiments showed that the absorption capacity of poisonous As by heat-treated agricultural products is directly proportional to the radical concentration in the bulk sample [1]. The higher the radical concentration, the larger the

absorption capacity. Therefore, γ -irradiation effect on the efficiency of absorption capacity would be expected. Fig.1 shows ESR intensity against the dose of γ -irradiation. It is apparent that original rice chaff (symbol A) is very strong against γ -irradiation, since its radical concentration is very low and is little affected. In the case of heat-treated rice chaff (~350 °C) (B), intensity became larger. Radical concentration increased gradually at lower doses and became saturated at higher doses. In green tea (C), the intensity much larger and the concentration increased linearly. From Fig.1, we can evaluate what kind of behavior is observed by heat-treatment and to what extent the radical concentration varies by γ -irradiation according to the difference of the kinds of agricultural products. Namely, in order to obtain some specified radical concentration one can understand what kinds of operation should be taken from a point of functional design of wasted agricultural products.

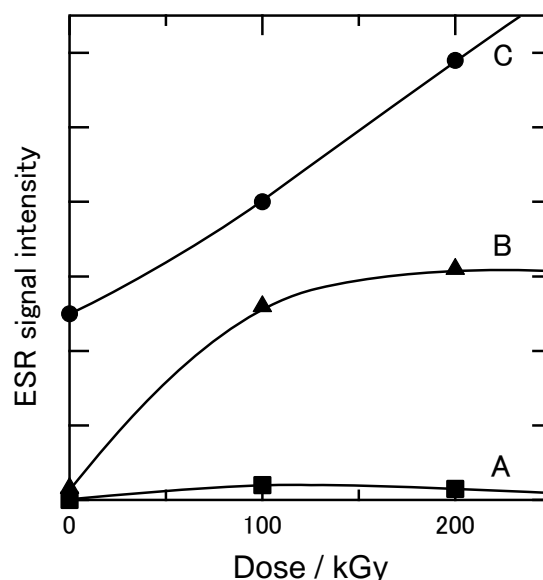


Fig.1 The effect of γ -irradiation on the signal intensity of ESR of three kinds of agricultural products (A, rice chaff; B, heat-treated rice chaff; C, Green tea).

REFERENCES:

[1] M. Minagawa, W. Katsumi, M. Shimizu, T. Matsuyama, N. Sato, to be published in Spring Conference of MLS Society, 2013.

Acknowledgement: Special thanks are expressed to Prof. T. Yoshiie for his kind help in EB experiments.

CO5-9 Measurement of Environmental Radioactivity and Heavy Metal in Seaweed Samples

T. Ohta, T. Kubota¹, Y. Mahara¹, T. Fujii¹, S. Fukutani¹, S. Sekimoto¹ and K. Takamiya¹

Faculty of Engineering, Hokkaido University

¹ Research Reactor Institute, Kyoto University

INTRODUCTION: The devastating tsunami caused by the great earthquake (Mw = 9.0) off the coast of northeastern Honshu on 11 March 2011 destroyed large areas along the coasts of Eastern Honshu in Japan. At Fukushima NPP, however, the standby power system was destroyed by the tsunami, disabling the cooling systems of the reactors. The loss of cooling resulted in the release of radionuclides, including ¹³¹I (T_{1/2} = 8.1 days), ¹³⁴Cs (T_{1/2} = 2.1 years), and ¹³⁷Cs (T_{1/2} = 30 years), into the atmosphere from the Fukushima NPP.

The iodine content in seawater consists mainly of two isotopes, ¹²⁷I and ¹²⁹I. ¹²⁹I (half-life 15.7 million years) is a radionuclide produced by cosmic-ray-induced spallation of Xe in the atmosphere and by spontaneous fission of uranium in the Earth's crust.

In the pre-nuclear era (i.e., before 1945), the ¹²⁹I/¹²⁷I ratio in natural seawater was reported to be less than 10⁻¹¹. However, after 1945, the amount of ¹²⁹I in seawater increased substantially owing to the release of this isotope from nuclear fuel reprocessing plants and nuclear weapons testing; consequently, the ¹²⁹I/¹²⁷I ratios in seawater and in marine algae have increased by several orders of magnitude compared to pre-1945 values.

In this study, we measured ¹²⁹I/¹²⁷I and ¹³⁷Cs in marine algae before and after Fukushima Nuclear disaster.

EXPERIMENTS: Seaweed samples were collected at Easter part of Japan from 2009 to 2011. (Fig. 1)

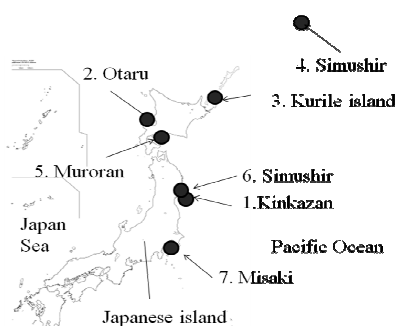


Fig. 1

2.1 Measurement of ¹³⁷Cs in algae samples by gamma-ray spectrometer

After seaweed samples were stored into U-8 plastic bottle and/or Steel container, Cs-137 in seaweed samples were measured by gamma-ray spectrometer (Isotope center, Hokkaido Univ.).

2.2 Neutron irradiation

About 10 – 100 mg of algal sample was sealed in clean plastic bag. The samples and reference standard samples were packed in an irradiation capsule. Neutron irradiation was carried out for 3-5 minutes using a pneumatic transport system (Pn-1) at the Research Reactor Institute, Kyoto University (KUR). After irradiation, γ -rays emitted from the samples were successively measured by a Ge detector. The iodine concentration in the samples was determined by counting γ -rays emitted from corresponding nuclides produced by (n, γ) reactions.

2.3 Measurement of ¹²⁹I/¹²⁷I ratio by AMS

The iodine isotopes ¹²⁷I and ¹²⁹I were isolated from marine algal samples to obtain ¹²⁹I/¹²⁷I ratios by means of accelerator mass spectrometry (Mutsu, JAEA, Japan, and Malt, Tokyo Univ.). The detailed separation and measurement of ¹²⁹I/¹²⁷I in seaweed was written by Mahara et al. and Ohta et al. [1,2].

RESULTS: The ¹³⁷Cs in seaweed samples in 2009 and 2010 were observed to be detection limit, while after Fukushima Nuclear disaster 66 Bq/kg in Ibaraki prefecture and 545 Bq/kg in Fukushima prefecture. The ¹²⁹I/¹²⁷I ratios observed in algae collected from 1928 to 1987 ranged from 10⁻¹³ to 10⁻¹⁰. The ¹²⁹I/¹²⁷I ratio in algae collected from 1987 was 100 - 1000 times as high as the ratio measured in algae from before 1945. This dramatic increase in ¹²⁹I/¹²⁷I ratio after 1945 was attributed to human activity.

REFERENCES:[1] Y. Mahara, T. Ohta, T. Tokunaga, H. Matsuzaki, E. Nakata, T. Nakano, T. Kubota, and H. Yasuda, Nucl. Instr. Meth. Phys. Res. B (2012) (accept). [2] T. Ohta, Y. Mahara, T. Kubota, T. Abe, H. Matsueda, T. Tokunaga, H. Matsuzaki, Nucl. Instr. Meth. Phys. Res. B (revise).

A part of this study is the result of “Kurashini manabu monodukuri” carried out under Sekisui Kogaku Co Ltd.

H. Nishido

*Research Institute of Natural Sciences,
Okayama University of Science,*

INTRODUCTION: Diamonds play a key role not only in material sciences, but also in the Earth and Planetary sciences. Natural and experimentally grown diamonds as well as their cathodoluminescence properties have been described from different origin such as metamorphic rocks, Chemical Vapor Deposition, High-Pressure High-Temperature (HPHT), Ultradispersive Detonation Diamonds (UDD), meteorites and meteoritic craters. They have clearly demonstrated that cathodoluminescence permits a rapid, non-destructive method of detecting defect symmetries in diamond samples from different origin.

Commonly, nanodiamond characterization has focused on chemical and physical properties with only limited luminescence spectroscopic investigations. In this study neutron implication experiments were conducted on graphite to clarify the formation mechanism of nanodiamonds by assuming neutron irradiation process at the KURRI. Here, we present the results of a study of scanning electron microscope-cathodoluminescence (SEM-CL) microscopy and spectroscopy of micro-and nanodiamonds from different origin. The purpose of these measurements is to investigate the capability of the SEM-CL technique to document temperature-related effects on diamond samples at room (RT) and liquid nitrogen (LNT) temperature, if there is a systematic difference in CL properties between diamond samples of different sources, to determine whether CL characteristics of diamond could be indicative of the astromineralogical application [1].

SAMPLES AND METHODS: The samples for CL measurements were mounted in two-component epoxy resin with non-luminescence. Their polished thin sections with 20 μm thickness were preliminary examined under a polarized microscope to clarify the textures indicating carbon materials. Their surfaces were finished using silicon colloidal with a grain size of 100 nm, and coated with amorphous carbon.

CL spectra were obtained using a scanning electron microscope-cathodoluminescence (SEM-CL), which comprises the SEM (JEOL: JSM-5410) combined with a grating monochromator (Oxford: Mono CL2). The SEM-CL system was operated at 15 kV accelerating voltage and a current of 1.5 nA. CL spectra were recorded in the range of 350-800 nm and a dwell time of 1 second per step by photon counting. All CL spectra were corrected for total instrumental response. Raman spectra were obtained from the polished samples using a laser Raman microscope (JASCO: NRS-2100) located at the KURRI.

RESULTS & DISCUSSION: Cathodoluminescence spectra of the natural diamond sample show a significant broad band centered at 541 nm at both room (RT) and liquid nitrogen (LNT) temperature. Compared to CL spectrum obtained at RT, an additional weak shoulder peak appears at 488 nm at the LNT with a relatively high peak intensity. The grain sizes of these diamond samples fall into a few hundred micrometers. The RT-CL spectrum of the synthetic diamond (HPHT) is dominated with a broad band centered at 540 nm, whereas the LNT-CL spectrum shows a broad band at 590 nm. Both CL spectra have two additional bands at around 445 (448 nm at RT and 444 nm at LNT) and 729 nm, which became dominant at the LNT spectrum.

The CVD diamond sample is dominated by a noisy broad band ranging from 370 to 400 nm in otherwise almost no CL spectral features obtained at room temperature. A broad band centered at 509 nm with a shoulder peak at 489 nm is dominant in the CL spectrum CVD specimen at LNT. The maximum grain size of these diamond samples is around 250 nm.

All CL spectra (RT) of the UDD samples are dominated by two broad bands at 388 and 462 nm, whereas spectra obtained at LNT exhibit only one but a significant broad peak, which is centered at around 540 nm. It is important to note that as a function of increasing size of the nanodiamond particles, there is a gradual change of the peak intensities. In contrast to the HPHT and CVD samples, CL spectrum of the meteoritic nanodiamond from Boroskino sample shows a broad band centered at 540 nm at RT.

The agglomerates are called A-Centers when occur as pairs of nitrogen atoms, which centered at around 390 nm in CL spectra, especially in type IaA diamonds. The B-centers as four nitrogen atoms surrounding a common vacancy and mixtures of them may also occur mostly in the type IaB diamonds. Type Ib – mostly represented in synthetic diamonds but very rare (about 0.1%) among natural diamonds – contain nitrogen as isolated single nitrogen atoms called C-Centers (centered at around 450 nm). In some cases, type I diamonds may also contain clusters of three nitrogen atoms called N3-Centers.

CL spectra from these nanodiamonds show substantial similarities but also some slight differences, whereas the assignment of emission bands at around 535 nm is not always straightforward, but corresponding to dislocation defects associated with nitrogen atoms. Although it was not possible to define exactly the aggregation status of nitrogen atoms, the CL spectra suggest a low concentration of nitrogen in the nanodiamonds and give some indications for distinguishing diamonds. A nitrogen content typically less than 20 ppm can be sufficient to provide the luminescence of diamond.

Reference:

[1] Gucsik, A, Nishido, H., Ninagawa, K., *Microscopy & Microanalysis* (in print).

Determination of the Uranium Content in Moldavite for the Absolute Evaluation of Fission-track Ages

T. Suzuki, K. Takamiya¹ and R. Okumura¹

Faculty of Education, Kagoshima University
¹ *Research Reactor Institute, Kyoto University*

INTRODUCTION: Absolute evaluation of fission-track ages for geological glasses instead of the so-called isothermal (or isochronal) plateau method or track-size correction method which uses the thermal annealing of fission tracks, have been tentatively applied to moldavite, a candidate age standard [1]. In this study, reactor neutron irradiation was employed only for uranium determination. Fission-track ages of moldavite and other glass materials can be calculated using the effective range of spontaneous fission tracks and the uranium content data. The effective range of tracks can be estimated from etch-pit parameters with the general etching rate for a polished surface according to the measurement of natural tracks on silicone replicas using a confocal laser ablation scanning microscope. These procedures allow the fission-track ages of geological glasses to be determined without direct handling of neutron-irradiated materials.

EXPERIMENTS: The uranium content of samples was estimated from normal fission-track analysis of separate fragments of samples using a polycarbonate external detector and IRMM-540R uranium monitor glass. Fission-track analysis remains an excellent and convenient method for uranium microanalysis of natural glasses. Moldavite samples collected from Jankov in southern Czech Republic were provided by Dr. G. Biggazzi (CNR, Pisa, Italy). Neutron irradiation was carried out using the pneumatic tube of TC graphite facility at the KUR Kyoto University Reactor (5 MW/h) for 2–4 h. Polished and nonirradiated moldavite samples were etched in 46% HF at 20°C for 15 min and polycarbonate films were etched in 6 N NaOH at 20°C for 12 min.

RESULTS: Examples of spontaneous fission tracks in moldavite and induced tracks on polycarbonate films are shown in Fig. 1 and Fig. 2. The uranium content of

moldavite determined in this study was 2.11 ± 0.04 and 2.21 ± 0.04 $\mu\text{g/g}$ for the two samples according to a comparison of track counting data between the samples and IRMM-540R monitor glass. The age of the moldavite was estimated at about 14 Ma using these uranium content data and etch-pit parameters. The results are in good agreement with the reference values and data obtained employing the normal fission-track method with the thermal annealing of tracks.



Fig.1. Spontaneous fission tracks in moldavite
Scale bar: 10 μm



Fig.2. Induced tracks on polycarbonate film
Scale bar: 10 μm

REFERENCES:

- [1] M.L. Balestrieri *et al.* in Van den haute, P. & De Corte, F. (eds.), *Advances in Fission Track Geochronology* (1998) 287–304. Kluwer Academic Publishers, Dordrecht.

N. Shirai, S. Sekimoto¹, S. Otsuka and M. Ebihara

Department of Chemistry, Tokyo Metropolitan University
¹Research Reactor Institute, Kyoto University

INTRODUCTION: Cations like Zr, Nb, Hf and Ta are relatively small in size and high in charge, and are grouped into high field strength elements (HFSE). Such elements pairs as Zr-Hf and Nb-Ta, which have similar ionic radius at the same valency states, are well known to behave in a similar way during igneous processes such as partial melting and fractional crystallization. As these elements are classified into refractory elements in cosmochemistry, element pairs represented by Zr-Hf and Nb-Ta behave similarly during cosmochemical processes. However, recent studies using improved analytical methods such as ICPMS indicate that the fractionations of Zr-Hf and Nb-Ta in cosmochemical and geological samples can occur [e.g., 1]. Therefore, Zr/Hf and Nb/Ta ratios provide useful information about condensation processes and igneous processes.

Various analytical methods represented by XRF, INAA, IPAA, ICP-AES and ICP-MS were applied for determination of HFSE. Among these analytical methods, ICP-MS has been increasingly used. There are some analytical problems when analytical method accompanying acid digestion such as ICP-MS is used. HFSE often involve in creating analytical problems such as incomplete acid digestion and instability in solution. As Nb is monoisotopic element, it is difficult to obtain accurate Nb values by using ICP-MS. In this study, we used IPAA for determination of Zr and Nb abundances for cosmochemical and geological samples. As IPAA is non-destructive methods, this is exempted from above-mentioned analytical problems for analytical method accompanying acid digestion. The aim of this study is to evaluate our Zr and Nb data for geological samples and cosmochemical samples compared with their literature values.

EXPERIMENTS: Five GSJ standards materials namely JA-2 (andesite), JB-1 (basalt), JB-3 (basalt), JG-1 (granodiorite) and JR-1 (rhyolite) were analyzed by IPAA. For cosmochemical sample, Allende meteorite was used. Chemical reagent sample, Fe₂O₃ (99.999 %, Soekawa Chemical Co., Ltd), was irradiated to correct the spectral interference of ⁵²Mn formed by the ⁵⁴Fe(γ ,pn)⁵²Mn reaction. For determination of Nb and Zr, SPEX solutions for Nb and Zr were dropped on the filter paper. Samples were taken into a sample container (9 mm ϕ) made of highly Al foil (Al: 99.5 %, Niraco Co., Ltd.). Five to ten samples were stacked, among which thin foil disk (9 mm ϕ) of Au as a monitor of the intensity of photon are placed. Samples in a block were put in a quartz tube. We used a linear electron accelerator at the

Research Reactor Institute, Kyoto University. Electrons were accelerated by the linear accelerator to about 30 MeV. After irradiation (about 30 hours), samples were taken into new Al foil and measured at the Laboratory of Radioisotopes, Tokyo Metropolitan University.

RESULTS: Niobium and Zr abundances were determined by using the 909.2 and 934.5 keV gamma-ray of ⁸⁹Zr and ^{92m}Nb, respectively. As reported by Kato and Matsumoto [2], 934.5 keV peak of ^{92m}Nb were caused by a spectral interference for 935.5 keV peak of ⁵²Mn. Its contribution was corrected by using 934.5 and 1434.1 keV peak of chemical reagent (Fe₂O₃). Contributions of ⁵²Mn were about 3 % for JB-1, 45 % for JB-3, 7 % for JA-2, 0 % for JR-1 and 8 % for JG-1. Our Zr and Nb abundances for five geological standard materials were compared with their reported values in Table 1. Our Nb and Zr values for five geological standard materials except for JB-3 are in good agreement with the corresponding reported values. Discrepancy for Nb of JB-3 is due to the relatively high spectral interference from ⁵²Mn. As shown in Table 1, there is difference of Zr abundance for JG-1 between ICP-AES and ICP-MS, and other methods. Analytical methods with acid digestion represented by ICP-AES and ICP-MS reported the lower Zr abundances in JG-1 compared with those of other methods. In consideration that granodiorites such as JG-1 contain zircon as accessory minerals and Zr is more partitioned into zircon than other minerals. As zircon is an acidic refractory material, it is hardly dissolved under acid digestion. As a result, Zr values from ICP-AES and ICP-MS are lower than those from other methods (e.g., IPAA). Our Zr values for JG-1 are significantly higher than literature values obtained from ICP-AES and ICP-MS and are consistent with reported values obtained from IPAA. Except for Nb for JB-1 and Zr for JG-1, the precision expressed as the relative standard is 4 % for Nb and Zr. The relatively high RSD for Nb of JB-3 is due to high spectral interference from ⁵²Mn. Our RSD value for Zr in JG-1 is higher. It is likely that zircon is heterogeneously distributed in JG-1.

Table 1. Analytical results for geological standard materials for Nb and Zr.

		JB-1	JB-3	JA-2	JG-1	JR-1
Nb (ppm)	This work*	36.4 (3.6)	1.95 (25)	9.16 (2.6)	12.9 (3.6)	15.1 (3.4)
	PAA	35.0	2.40		12.0	16.9
	ICPES	32.9	2.73	9.30	10.2	16.1
	ICPMS	34.91	2.10	9.27	11.5	15.3
	XRF	30.5	2.58	9.33	12.4	15.1
Zr (ppm)	This work*	134 (1.9)	87.5 (0.7)	104 (0.4)	138 (20)	105 (3.6)
	PAA	134	88.8		135	102
	ICPES	146	96.4	120	59.2	93.7
	ICPMS	135	95.5	110	27.7	98.1
	INAA	168	93.5	111	135	127
	XRF	147	96.5	114	113	100

*The values in brackets are RSD (n = 3).

REFERENCES:

- [1] C. Münker *et al.*, Science, **301** (2003) 84-87.
- [2] T. Kato and K. Matsumoto Geostand. Newsl., **5** (1981) 167-170.

Determination of Iron and Manganese in the Sediments under Hypoxia with High Time Resolution

K. Shozugawa, T. Okoshi, T. Yamagata, R. Okumura¹, K. Takamiya¹ and M. Matsuo

Graduate School of Arts and Sciences, The University of Tokyo

¹*Research Reactor Institute, Kyoto University*

INTRODUCTION: Hypoxia, known as dead zones with little dissolved oxygen (DO) in the bottom water mass, has expanded since the 1960s on sea coasts all over the world and has greatly influenced ecosystems and in-shore fisheries [1]. At the seabed in Tokyo Bay, vast dredged trenches have been formed sporadically along the coasts by reclamation of the foreshore since the 1970s [2]. Although the water depth of the coastal Tokyo Bay is from 5 to 10 meters, the water depth of some dredged trenches reaches 30 meters. In particular, the dredged trench off Makuhari has the maximum area and depth, and strong hypoxia has been observed there due to the stagnation of water currents. In this study, sediment cores were collected from the Makuhari dredged trench and concentrations of iron and manganese in sediments were analyzed by activation analysis with high time resolution.

EXPERIMENTS: In the dredged trench (station OC and OD, water depth was over 25 m), the seabed was muddy and DO level of bottom water was $0 \text{ mg}\cdot\text{L}^{-1}$ under 5 m. In contrast, the non-dredged seabed (station OE, water depth was less than 10 m) was sandy. Both cores were cut in the vertical direction at 0.6 - 3.0 cm intervals after freezing. 50mg of dried (110°C , 2 hours) sediments were packed in double polyethylene film bags. All samples were irradiated at the pneumatic tube, Kyoto University Reactor (KUR). Gamma-ray measurements were applied to 2 methods depending on half-lives of ^{56}Mn and ^{59}Fe . For analysis of ^{56}Mn , samples were irradiated for 10 seconds at 1MW, and then gamma-ray was measured for 600 seconds (live time) by Ge detector. Regarding ^{59}Fe , irradiated for 20 min at 1MW. Measurement time of gamma-ray of ^{59}Fe was for 9000 seconds (live time) after 2 weeks cooling.

RESULTS: Figure 1 shows the DO in the bottom water at dredged area and at an observatory (non-dredged) near the Tokyo light beacon. Seawater above the dredged trench had the following features: 1) vertical circulation is weak in summer, and 2) horizontal currents are the same as in other areas. That is, the Makuhari dredged trench underwent a localized low DO event caused by rapid DO consumption such as microbial respiration. It is well-known fact that concentrations of iron and manganese in sediments have increased when condition of sea-

water is oxidative condition, i.e. winter season, on the other hand, concentrations have decreased due to eluviations of Fe^{2+} and Mn^{2+} when condition of seawater is anoxic like hypoxia. Figure 2 shows vertical distributions of iron and manganese in the sediments collected at both dredged and non-dredged area. Each layer corresponds to ca. 0.5 year age of sedimentation. At station OC (●) and OD (■) which were dredged area, concentrations of both elements decreased near the surface. On the other hand, at station OE (Δ) which was non-dredged area, concentrations of both elements were almost constant at the surface. During the sampling periods, it was such anoxic condition that blue tide had occurred all over the coast of Tokyo bay. This fact indicated that strong hypoxia occurred at dredged area had been recorded at the surface of sediments.

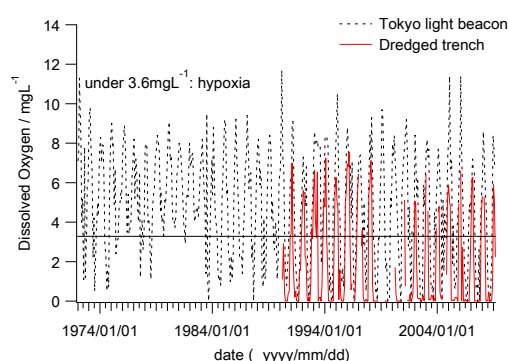


Fig. 1. Variation in DO of bottom water mass over decades in the dredged area (full) and the Tokyo beacon (dashed).

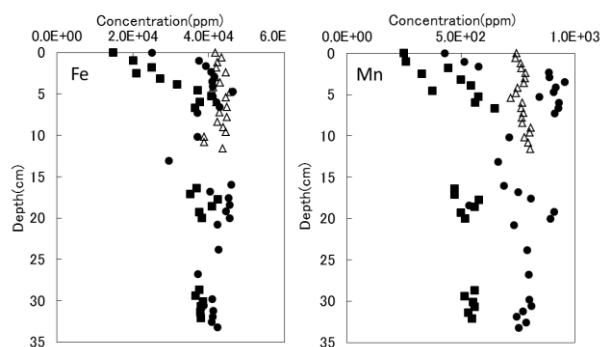


Fig. 2. Vertical distribution of Fe (left) and Mn (right) in the sediments. Stations OC (●) and OD (■) were located at dredged area, station OE (Δ) was located at non-dredged area.

REFERENCES:

- [1] Diaz R.J., Rosenberg R., *Science*, **321** (2008) 926-929.
 [2] Sasaki, J., Kawamoto, S., Yoshimoto Y., Ishii, M. Kakino, J., *J. Coastal Res.*, **56** (2009) 890-894.

CO5-14 Instrumental Neutron Activation Analysis of Crystalline Schist Boulders from the Upper Cretaceous Onogawa Group, Eastern Kyushu, Japan

T. Suzuki, K. Takamiya¹ and R. Okumura¹

Faculty of Education, Kagoshima University

¹ Research Reactor Institute, Kyoto University

INTRODUCTION: Metamorphic rock of crystalline schist ranging from boulders to pebbles have found in the Upper Cretaceous Onogawa Group [1, 2] which is developed closely with Sanbagawa metamorphic rock in eastern Kyushu, south-western Japan. However, Isozaki and Itaya [3] used K-Ar dating to determine the Early Jurassic ages of two boulders of these schist clasts and suggested that the boulders were derived not from Sanbagawa but from Sangun metamorphic rocks. Other while, several recent studies have insisted that Sanbagawa metamorphic rocks are metamorphic facies of the Lower Shimanto Group [4]. The purpose of this study is to clear the chemical characteristics of crystalline schist boulders in the Upper Cretaceous Onogawa Group, psammitic Sanbagawa metamorphic rock, psammitic rock of the Cretaceous Shimanto Groups and psammitic Sangun metamorphic rock with the rocks from Asaji, Asakura and Nagasaki in northern Kyushu.

EXPERIMENTS: Instrumental neutron activation analysis is a convenient and accurate method of multielemental analysis for a large number of geological samples. Neutron irradiation was carried out using the Pn-2 facility at KUR Kyoto University Reactor (1 MW/h) for 1–2 h. Gamma-ray spectrometry was conducted at the Radio Isotope Laboratory of Kagoshima University. In all, 106 irradiated samples made from 39 rock specimens and working standards of GSJ JB1a and JR1 were analyzed.

RESULTS: Because the analysis reported in this study is still underway owing to the long life of the nuclides, partial experimental results are presented here with the data already given for the Shimanto Group as the average values for about 100 samples. Figure 1 shows the relation between the abundance of La and that of Th normalized by the Sc content. Figure 2 shows the lanthanoid pattern for the rocks analyzed. The Sanbagawa crystalline schist boulders in this study are

slightly pelitic.

From the data of the trace element abundance, the origin of crystalline schist boulders in the Onogawa Group remains unclear. Further investigations using additional samples and parameters are required.

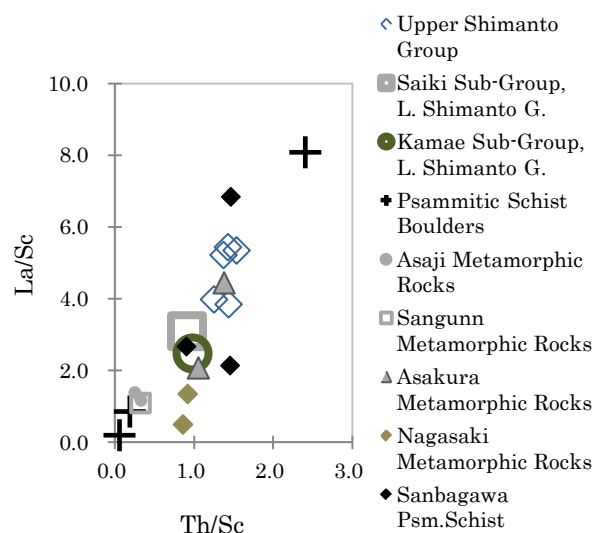


Fig.1. Relation between La/Sc and Th/Sc.

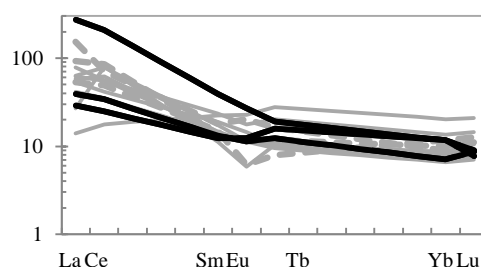


Fig.2. Lanthanoid pattern of psammitic rocks.
Bold line: Crystalline schist boulders in the Upper Cretaceous Onogawa Group.

REFERENCES:

- [1] N. Kanbe and Y. Teraoka, *Geology of the Usuki district*, Geol. Surv. Japan (1968), 40p.
- [2] K. Miyazaki and T. Yoshioka, *Geology of the Saganoseki district*, Geol. Surv. Japan (1994), 63p.
- [3] Y. Isozaki and T. Itaya, *Jour. Geol. Soc. Japan*, **95** (1989) 361–368.
- [4] S. Otoh *et al.*, *Jour. Geogr.*, **119** (2010) 333–346.

CO5-15 Natural Analogue Study Using Trace Elements in Rock Alteration Zones

T. Honda, T. Hagiwara and S. Sekimoto¹
 Graduate School of Engineering, Tokyo City University
¹Research Reactor Institute, Kyoto University

INTRODUCTION: High level radioactive waste (HLW) can remain highly radioactive for tens of thousands of years. As a method of HLW disposal, geologic disposal has been employed in Japan. Under this method, it is assumed that the radioactive substances included in HLW will be contained by an artificial barrier for several thousand years and by a natural barrier for tens of thousands of years thereafter. Some observers, however, have pointed out safety issues. In deep strata, groundwater generally flows slowly but, in cases in which such strata has many fractures and faults, can flow quite rapidly, raising concern that radionuclides can leach into the environment sooner than expected. In this study, we evaluate the distribution and behavior of natural analogue elements in altered rocks. We examine the trace elements uranium (U), thorium (Th), and the lanthanoids as natural analogues to minor actinoids. The chemical properties of the lanthanoids are similar to those of minor actinoids, such as americium (Am) and curium (Cm); by understanding the behavior of these analogues in altered rock over long periods, we should thus be able to evaluate the likely behavior of minor actinoids under similar conditions.

EXPERIMENTAL:

Seven rock samples were collected from boreholes drilled under the direction of researchers from the Tono Geosciences Center of the Japan Atomic Energy Agency. Sample examination, primarily macroscopic observation, centered on feldspar and biotite alteration zones. Non-alteration and alteration zones were identified in this manner (Table 1). Trace elements, namely, U, Th, and the lanthanoids, were measured by neutron activation analysis (NAA) of pulverized samples. Neutron irradiation was performed at the Kyoto University Research Reactor (KUR; Table 2).

Table 1. Profile of samples

Group	Samples	Lithofacies
TG1	TGP1-1-1	Parent
	TGP1-1-2	Parent
	TGP1-2	Parent
	TGP1-3	Parent
TG2	TGA2-1	Alteration
	TGA2-2	Alteration
	TGA2-3	Alteration
TG3	TGP3-1	Parent
	TGP3-2	Parent
	TGP3-3	Parent
TG4	TGP4-1	Parent
	TGP4-2	Parent
TG5	TGA5-1	Alteration
	TGA5-2	Alteration
TG6	TGA6-1	Alteration
	TGA6-2	Alteration

Table 2. Irradiation conditions at KUR

Half-life	Irradiation facility	Output (MW)	Max thermal neutron flux (n/cm ² ·s)	Irradiation time
long	PN-2	1	5.5×10 ¹²	4h
short	PN-3		4.68×10 ¹²	40sec.

RESULTS: Similar results were obtained for all samples except for those in the TG2 group. Light lanthanoids (lanthanum (La) to europium (Eu)) were found to be in-

corporated into mainly silicate minerals but also incorporated to some degree into oxide or carbonate minerals. Heavy lanthanoids (gadolinium (Gd) and lutetium (Lu)) were found to be incorporated into mainly silicate minerals but also partly into oxide etc.. U and Th were found to behave similarly to the heavy lanthanoids. As for the TG2 group samples, it is thought that light lanthanoids are incorporated into mainly oxide (and into sulfide and phosphate minerals in the case of TGA2-2 only), with some slight incorporation into carbonate minerals. Heavy lanthanoids were found to be incorporated into mainly silicate minerals. However, the abundance of heavy lanthanoids in silicates was lower than that in the parent rock, and the abundance in other minerals (oxide, carbonate minerals) increased. U and Th were found to behave similarly to the heavy lanthanoids.

From the above, in the alteration zones, the abundance of lanthanoids is lower in silicates than in other minerals. Therefore, it is possible that lanthanoids precipitated in the alteration zone upon an infusion of lanthanoid-bearing groundwater.

We next consider the behavior of minor actinoids in light of the above findings regarding their natural analogues. Lanthanoids were found to be contained in clay and carbonate minerals formed by alteration. Clay has a layered structure; and, as each layer is negatively charged, cations are thus drawn to them. Many radioactive substances (Am, Cm, etc.) are positively charged. It has been reported that radioactive substances are incorporated into clay through ion exchange. Indeed, we find that light lanthanoids had been incorporated into clay within the alteration zones. Because the ionic radii of light lanthanoids (98 to 122 pm) are similar to those of Am and Cm (107 and 99 pm), we infer that those two elements are also readily incorporated. In addition, it has been reported that light lanthanoids are also readily incorporated into carbonate minerals because the ionic radii of those elements are similar to that of the carbonate constituent Ca²⁺ (106 pm)¹. This is consistent with our finding that light lanthanoids are incorporated into the carbonate minerals within both the alteration zones and the parent rock. Because light lanthanoids are readily incorporated into carbonate minerals, we infer that Am and Cm are likewise readily incorporated into those minerals. We also found that light lanthanoids are incorporated into oxide and phosphate minerals, leading us to infer that Am and Cm are also incorporated into oxide and phosphate minerals. We also found that many light lanthanoids accumulate in alteration zones. From this we infer that Am and Cm similarly accumulate in alteration zones.

REFERENCES:

[1] R. Dobashi *et al.*, *Geochemistry*, **42** (2008)79.

S. Miyata, Y. Matsumoto, H. Sakane, K. Takamiya¹
and R. Okumura

Graduate School of Science, Kyoto University
S.H.I. Examination & Inspection, LTD.

¹Research Reactor Institute, Kyoto University

INTRODUCTION: Neutron Activation Analysis (NAA) in Japan has been performed mainly at KUR of Kyoto University Research Reactor Institute and JRR-3 of Japan Atomic Energy Agency. However, a comparison between sensitivities in performing NAA with KUR and that with JRR-3 had not been discussed. Then we carried out comparison experiments for stabilities of neutron flux and neutron spectrum. And examinations of determining the standard material of NIST SRM 1633b were performed by k_0 -NAA between KUR and JRR-3 for an analysis of air particulate matter [1].

EXPERIMENTS: Gold standard foils were irradiated for 3 minutes at Pn-3 to evaluate neutron flux deviation by every 10 min. And Au and Zr standard foils were irradiated together for 5 minutes at Pn-3 for evaluate neutron energy spectrum. About 1 day after irradiation, the Au and Zr standards were measured for 150 and 5000 seconds, respectively. The neutron flux deviation of Pn-3 were evaluated from activity of Au standards, and neutron energy spectrum were evaluated from the value of f (rate of thermal/epithermal neutron fluxes) and α (deviation of neutron energy spectrum from $1/E$) calculated by triple monitor method. NIST SRM1633b was irradiated for 1 minute by Pn-3 (1MW) for measurements of short lived nuclides, and 40 minutes by Pn-2 (5MW) for measurements of long lived nuclides. Interference correction from nuclear reaction of $^{27}\text{Al}(n, p)^{27}\text{Mg}$, $^{27}\text{Al}(n, \alpha)^{24}\text{Na}$, and $^{56}\text{Fe}(n, p)^{56}\text{Mn}$ were carried out using results obtained by irradiation experiments for pure Al and Fe samples.

RESULTS: The relative standard deviations of neutron fluxes at Pn-3 KUR are 1.5% (Fig. 1a) and 1.8% at PN-3 in JRR-3 (Fig. 1b), which means neutron flux deviation at Pn-3 of KUR is similar level as PN-3 of JRR-3. The deviations of f and α values are 22% and 166% in KUR, respectively. In JRR-3, f deviation is 6.4%. It shows that the neutron energy spectrum at Pn-3 of KUR is more unstable than that at PN-3 of JRR-3. Difference between determined values and certified values of NIST SRM1633b was within 10% in 20 elements (Fig.2)

CONCLUSION: The stabilities of neutron fluxes at neutron irradiating position of KUR and JRR-3 are simi-

lar, but the neutron energy spectrum at Pn-3 of KUR was more unstable than that at PN-3 of JRR-3. And differences between determined values and certified values of NIST SRM1633b are within 10% for 20 elements. Although energy spectrum was unstable in comparison with JRR-3, qualitative analysis by k_0 -NAA method using KUR is available.

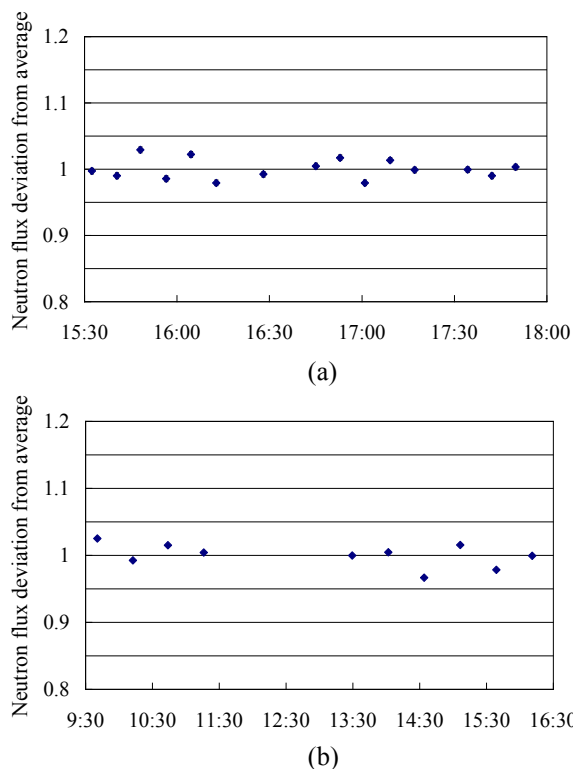


Fig. 1. Neutron flux deviation from average about KUR(a) and JRR-3(b).

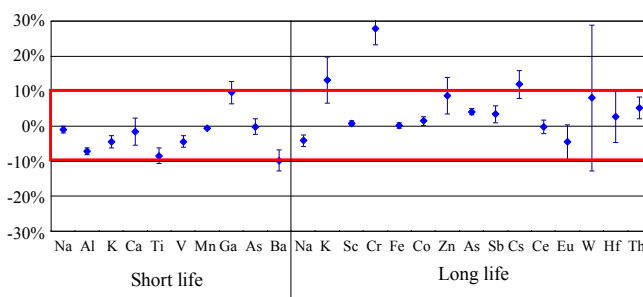


Fig. 2. Deviation of analytical results from certified value.

REFERENCES:

[1] S. Miyata *et al.*, *Bunseki kagaku*, **689** (2006)

Geochemical Mapping for the Upper Ara-river System Area, Saitama Prefecture by Neutron Activation Analysis

T. Fukuoka, Y. Saito¹, M. Ishimoto² and H. Kusuno

Faculty of Geo-environmental Science, Rissho University

¹*College of Science and Engineering, Aoyama Gakuin University*

²*School of Engineering, The University of Tokyo*

INTRODUCTION: Geochemical maps can express areal distributions of chemical elements in the earth's land surface and give information about the chemical background in the natural environment to assess the artificial environmental changes [1, 2]. In this study, we report the geochemical mapping for the upper Ara-river system, Chichibu Mountains area, Saitama in 2011. Cosmo-Geochemistry Lab., Rissho University has been making up the geochemical maps since 2000.

EXPERIMENTS: We analyzed the stream sediments which had been collected as a sample representing the geochemical characters in each drainage basin. A sampling site 1 per 1 km² was selected in the area which a mountain ridge was surrounding and at 100m upper stream in the branch from the junction of main stream to avoid the contamination by floods. The stream sediment was sieved to 80 mesh (<180 μm) on site and the fine fraction was reserved for analysis. 47 elements in collected samples are analyzed by X-ray Fluorescence Analysis (XRF), Laser Ablation Inductively Coupled Plasma Mass Spectrometry (LA-ICP-MS), Prompt Gamma-ray Analysis (PGA) and Instrumental Neutron Activation Analysis (INAA) (Fig. 1 and 2). INAA has great advantage for Au, As and Sb analyses compared with ICP-MS, because of their high ionization potential.

RESULTS: Figure 3 indicates as an example of geochemical map of Au resulted from this study. In previous studies of geochemical map of this area, western area indicate highest contents of Au, As and Sb. The geochemical maps of As and Sb indicate similar distribution of these elements and similar to Au. Gold mine was operated formerly in this area.

In this study, we found new high Au content point (No. 1121 point in Fig.3). In this sampling point, Au content is surprisingly high, but As and Sb contents are normal. So, we have to clear the reason why it doesn't agree with geochemical behavior of three elements, in No. 1121 sampling point. Possible answer is analytical contamination. Because recently Au distributes widely in our living environment such as cosmetics, electrical connector etc.

Fieldwork to collect samples

↓
Dehydration of samples
at room temperature

↓
110°C

↓
900°C

1.3 g

XRF
LA-ICP-MS

0.7 g

PGA

Fig. 1 Flowchart of analytical procedure.

	1	2	3	4	5	6	7	8	9	10	#	12	13	14	15	#	17	18	
1	H																		He
2	Li	Be											B	C	N	O	F	Ne	
3	Na	Mg											Al	Si	P	S	Cl	Ar	
4	K	Ca	Sc	Ti	V	Cr	Mn	Fe	Cu	Ni	Cd	Zn	Ga	Ge	As	Sb	Br	Kr	
5	Rb	Sr	Y	Zr	Nb	Mo	Tc	Ru	Rh	Pd	Ag	Cd	In	Sn	Sb	Te	I	Xe	
6	Cs	Ba	LA	Hf	Ta	W	Re	Os	Ir	Pt	Au	Hg	Tl	Pb	Bi	Po	At	Rn	
7	Fr	Ra	AC																
			LA	La	Ce	Pr	Nd	Pm	Sm	Eu	Gd	Tb	Dy	Ho	Er	Tm	Yb	Lu	
			AC	Ac	Th	Pa	U	Np	Pu	Am	Cm	Bk	Cf	Es	Fm	Md	No	Lr	

XRF
 LA-ICP-MS
 INAA
 PGA

Fig. 2 Elements analyzed by XRF, LA-ICP-MS, PGA and INAA.

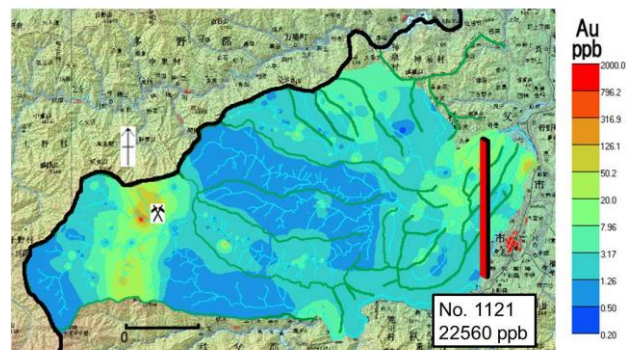


Fig. 3 The gold geochemical map of the upper-Ara River System.

REFERENCES:

- [1] Darnley, A. G. et al. (1995) 19, UNESCO Publishing, Paris.K.
- [2] Johnson, C. C., Brown, S. E. and Lister, T. R. (2003) Internal Report, IR/03/096N. British Geological Survey, Keyworth, Nottingham.